

1

1 **Title:**
2 The Goldilocks Window of Personalized Chemotherapy: An
3 Immune Perspective

4 **Authors and Affiliations:**

5 Derek S. Park^{1,2}, Mark Robertson-Tessi², Philip K. Maini³, Michael B. Bonsall¹, Robert A.
6 Gatenby^{2,4}, Alexander R. A. Anderson²

7 1 – Department of Zoology, University of Oxford, Oxford, United Kingdom

8 2 – Department of Integrated Mathematical Oncology, H. Lee Moffitt Cancer Center, Tampa,
9 Florida, United States of America

10 3 – Mathematical Institute, University of Oxford, Oxford, Oxfordshire, United Kingdom

11 4 - Department of Radiology, H. Lee Moffitt Cancer Center, Tampa, Florida, United States of
12 America

13

14 **Corresponding Authors:**

15

16 Derek Park
17 12902 USF Magnolia Drive
18 Mailstop: SRB 4
19 Tampa, FL 33612
20 Derek.park@aya.yale.edu

21

22 Alexander R. A. Anderson
23 12902 USF Magnolia Drive
24 Mailstop: SRB 4
25 Tampa, FL 33612
26 Alexander.anderson@moffitt.org

27

28 **Running title:**

29 The Goldilocks Window of Personalized Chemotherapy

30

31 **Keywords:**

32 Personalized medicine, tumor-immune interactions, chemotherapy, scheduling, T-cells

33

34 **Conflict of Interest statement:**

35 The authors declare no potential conflicts of interest.

36 **Abstract**

37

38 The immune system is increasingly being recognized for its untapped potential in being
39 recruited to attack tumors in cancer therapy. The main challenge, however, is that most tumors
40 exist in a state of immune tolerance where the patient's immune system has become
41 insensitive to the cancer cells. In order to investigate the ability to use chemotherapy to break
42 immune tolerance, we created a mathematical modeling framework for tumor-immune
43 dynamics. Our results suggest that optimal chemotherapy scheduling must balance two
44 opposing objectives: maximal tumor reduction and preserving patient immune function.
45 Successful treatment requires therapy to operate in a 'Goldilocks Window' where patient
46 immune health is not overly compromised. By keeping therapy 'just right', we show that the
47 synergistic effects of immune activation and chemotherapy can maximize tumor reduction and
48 control.

49

50 **Statement of Significance**

51

52 In order to maximize the synergy between chemotherapy and anti-tumor immune response,
53 lymphodepleting therapy must be balanced in a 'Goldilocks Window' of optimal dosing.

54

55

56 Introduction

57

58 By the time a tumor is clinically detectable, it is no longer subject to significant anti-tumor response
59 from the innate and acquired components of the host immune system. Mechanistically, this immune
60 tolerance is the result of complex interactions among tumor cells, T cells, and secreted cytokines [1].
61 CD8+ effector T cells, also known as cytotoxic T lymphocytes (CTLs), are an important component of the
62 adaptive immune system that responds to tumor antigens and induces cell death.

63 A major barrier to effective CTL response in tumors is suppression by T regulatory cells (Tregs),
64 which inhibit CTL cytotoxic activity via cell-cell contact ([2], [3]) as well as through secreted factors such
65 as TGF-beta ([4] [5]). They have posed challenges for cancer immunotherapies as well as preventing the
66 activation of the immune system during more traditional therapy approaches ([3], [6]). Tregs also
67 appear to play a critical role in limiting immune response in maternal tolerance of the fetus and
68 protection of commensal bacteria from the host immune system [2].

69 Multiple methods have been investigated to break the immune system from tolerance and
70 revive anti-tumor immune activity. The initial focus of these approaches included activation of CTLs
71 through immunostimulatory cytokines such as interleukin-2 (IL-2). More recently, lymphodepleting
72 chemotherapy has been recognized to have paradoxical but important immunostimulatory effects.
73 Heavy lymphodepletion has been reported to enhance the impact of adoptively transferred tumor-
74 specific T cells ([7]). This leads to the interesting question of whether or not lymphodepletion can also
75 enhance the efficacy of existing T-cell populations to mount an anti-tumor response. While
76 Gemcitabine, 5-Fluorouracil and other cytotoxic drugs can initially suppress immune subpopulations,
77 notably B and T cells, the subsequent proliferation of the immune cells when therapy is completed
78 provides a transient period in which immune response to tumor antigens can be restored. An obvious
79 question then arises: is there a better chemotherapy schedule that could maximize tumor kill and also
80 enhance immune response?

81 To investigate the dynamics of this transient immune response following chemotherapy, we
82 created a mathematical model of the complex tumor-immune dynamics that occur during multiple
83 cycles of chemotherapy. In particular, we investigated three, clinically-relevant, therapeutic dynamics:
84 immunodepletion, immunostimulation via vaccination, and immunosupportive prophylactics. We
85 identified significant immune trade-offs during chemotherapy as well as the relevant patient metrics
86 that determine the magnitude and severity of these compromises. Further, by exploring the impact of
87 clinically-established, as well as more experimental treatment, decisions we illustrate a more complex
88 interplay between chemotherapy and patient immune dynamics than has been previously investigated.
89 Our results indicate that optimal chemotherapy requires identification of a 'Goldilocks Window' in which
90 treatment can both induce cytotoxic effects in the tumor and enhance the immune response to tumor
91 antigens. Therefore, instead of the one-size-fits-all paradigm of fixed therapy regimens, patient immune
92 biology should be a key consideration when developing personalized chemotherapy strategies.

93 Methods

94

95 **Quick guide to equations and assumptions:**

96

$$\frac{dT}{dt} = \frac{T}{T^*(T)} - k_0 \frac{TE}{T+E} \left(1 - B \frac{R}{R+E}\right)$$

$$\frac{dE}{dt} = H(t_{off} - t) \left(1 - \frac{M+N}{K_{max}}\right) \gamma \alpha \frac{TM}{T+M} - H(t - t_{off}) \delta_E E \left(1 + c \frac{R}{R+E}\right) - \rho E$$

97

$$\frac{dM}{dt} = r_M M \left(1 - \frac{M+N}{K_{max}}\right) - H(t_{off} - t) \left(1 - \frac{M+N}{K_{max}}\right) \alpha \frac{TM}{T+M} + H(t - t_{off}) \delta_E \omega E$$

$$\frac{dR}{dt} = \sigma T - \delta_R R$$

$$\frac{dN}{dt} = r_N N \left(1 - \frac{M+N}{K_{max}}\right)$$

98

99

100 Our model assumes that tumor cells (T) grow unless checked by T effector cells (E). However, effector
 101 cells are themselves inhibited by T regulatory cells (R) that are recruited at a rate σ by tumor antigens.
 102 This leads to effector-cell-mediated tumor cell death being moderated by the quantity of T regulatory
 103 cells $\left(\frac{R}{R+E}\right)$. Effector cells exhibit different behaviors during immune expansion and immune contraction.
 104 This switching behavior is modeled with the Heaviside function $\left(H(t_{off} - t)\right)$. During the immune
 105 expansion phase, effector cells are recruited based on both available memory cells (M) and the tumor
 106 burden $\left(\frac{TM}{T+M}\right)$. Memory cells are the pool of T cells from which effector cells are derived. During
 107 immune expansion, the antigenicity of the tumor (α) induces differentiation to effector cells $\left(\frac{TM}{T+M}\right)$.
 108 However, as immune tolerance sets in, there is a contraction in the effector T cell population. This is
 109 caused by degradation of effector cells by T regulatory cells $\left(1 + c \frac{R}{R+E}\right)$. During immune contraction,
 110 there is also a small influx into the memory T cell compartment due to conversion of effector cells to
 111 memory T cells (ωE). Finally, the total lymphocyte population is represented by naïve cells (N) which
 112 replicate in a logistic growth model $\left(1 - \frac{M+N}{K_{max}}\right)$.

113

114 Overall Model Design

115

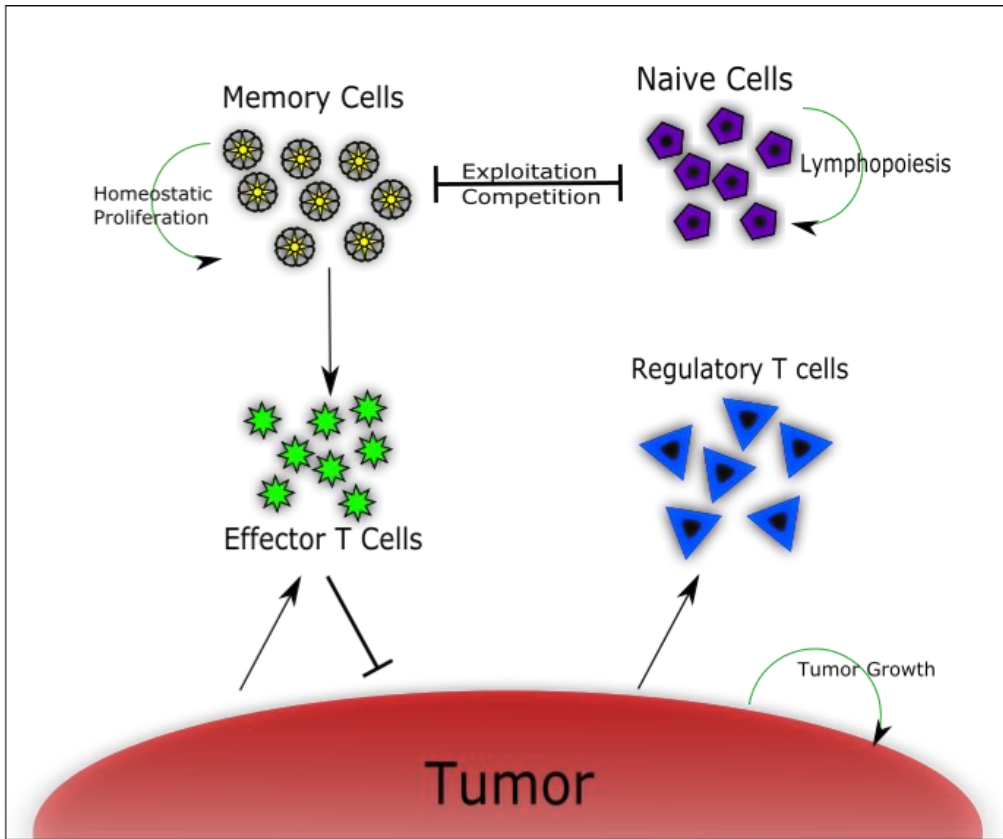
116 A central assumption of this work is that a clinically-detectable tumor has induced a tolerant
 117 state in which the immune system can no longer respond to tumor antigens. Chemotherapy temporarily
 118 removes this tolerance through lymphodepletion, which eliminates Tregs and allows a burst of immune
 119 response. However, the lymphodepletion itself also kills CTLs and therefore reduces the potential
 120 cytotoxic efficacy. This double-edged response to chemotherapy implies that there is an optimal
 121 therapeutic strategy. If the dose is too high, then the few remaining immune cells will not be able to
 122 take advantage of the tolerance breaking; if the dose is too low, then the immune depletion will be
 123 insufficient to break tolerance. In addition to these immune effects, the chemotherapy itself can induce

124 cancer cell death affecting both the tumor size directly and releasing tumor antigens, adding another
125 layer of complexity to the tumor-immune dynamics.

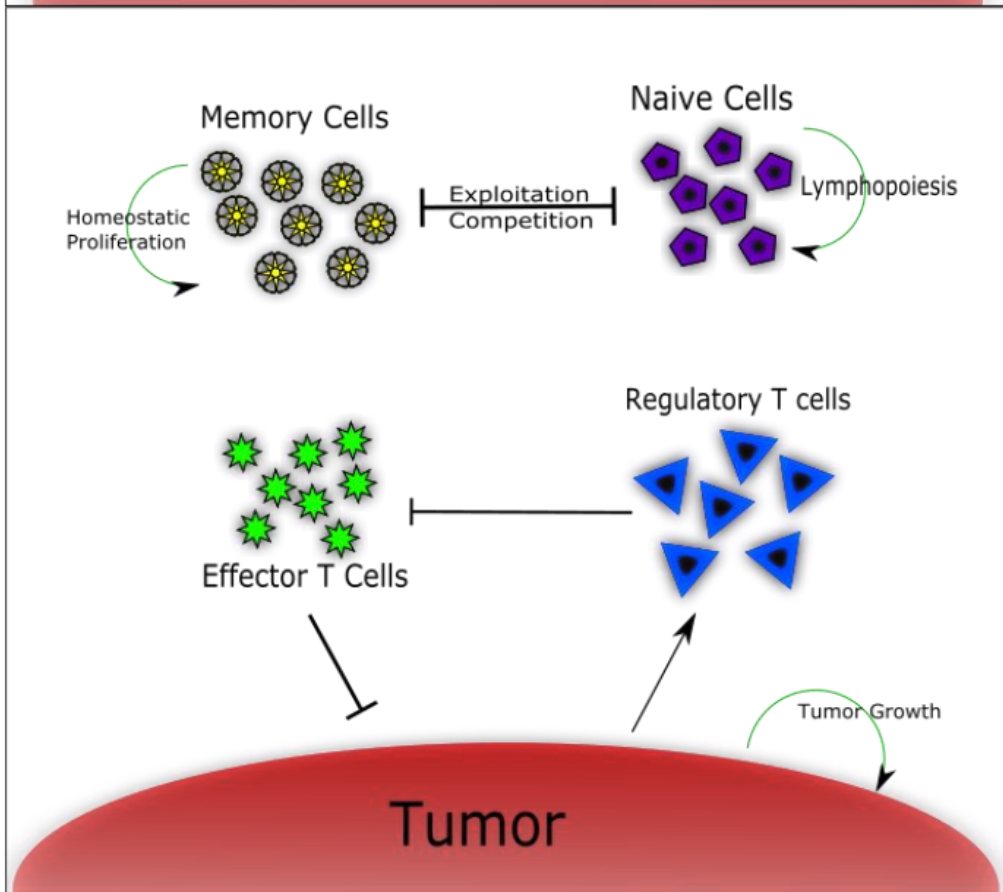
126 We develop a mathematical model that includes five major populations of cells: Tumor cells (T),
127 T effector cells (also known as cytotoxic T lymphocytes, CTLs, and denoted as E), T regulatory
128 cells (Tregs, R), Memory T cells (M), and Naive T cells (N). Immune function is separated into two distinct
129 temporal stages relative to the time of application of each chemotherapy cycle: 1) a period of CTL
130 expansion in a sensitized immune system, immediately following the application of chemotherapy
131 (Figure 1, panel A), and 2) CTL contraction as tolerance returns (Figure 1, panel B). The transition
132 between these expansion and contraction phases is governed by mechanisms that remain poorly
133 characterized, but empirically occurs 5-10 days after the expansion starts [8]. In the model, the
134 transition time is set to 5 days after the start of the immune expansion phase. Therefore, there is a
135 window of 5 days immediately following each cycle of chemotherapy in which the immune system is
136 sensitive, and outside of these periods, it is tolerant.

6

A



B



138 **Figure 1:** Tumor-immune dynamics during the sensitive (A) and tolerant (B) stages of the
 139 immune response. During antigen-sensitive immune expansion, CTLs are recruited from memory cells to
 140 attack tumor cells. Tregs are being recruited but have not yet started significantly inhibiting CTL
 141 responses. During immune contraction once tolerance sets in, Tregs exert an active inhibitory pressure
 142 on CTLs. Expansion of memory cells into CTLs ceases. Both stages of the immune response are
 143 characterized by competition between memory and naïve immune cells for common cytokine pools as
 144 well as homeostatic proliferation and lymphopoiesis.

145
 146
 147 During the phase in which the immune system is sensitive to the tumor, a few key processes
 148 occur. CTLs, which target and kill the tumor, are recruited from a memory cell population due to
 149 detection and response to tumor antigens [8]. These memory cells are constantly undergoing a low level
 150 of replenishing proliferation, but they only convert to CTLs during the sensitive expansion phase
 151 following lymphodepletion. During this phase, there is also tumor-mediated recruitment of Tregs. This
 152 eventually causes a significant shift in immune dynamics, leading to a contraction of the effector
 153 compartment during the tolerized phase. Under tolerance, there is no longer a significant recruitment of
 154 effector cells from the memory cell compartment. Instead, while the existing effector cells do carry out
 155 some tumor-killing function, the Tregs decrease the CTL number.

156
 157 **Tumor dynamics**

$$\frac{dT}{dt} = \underbrace{\frac{T}{T^*}}_1 - \underbrace{k_0 \frac{TE}{T+E} \left(1 - B \frac{R}{R+E}\right)}_2 \quad (1)$$

158 Tumor growth dynamics are approximated via a combination of exponential growth for smaller tumors
 159 and power law growth for larger tumors, as shown in the first term on the right hand side of Eq. (1). The
 160 transition between these growth dynamics is governed largely by the T^* term as defined in equation (2),
 161 following the implementation of tumor-immune growth dynamics described in [9].

$$T^* = \left(\left(\frac{1}{T_{trans}^{m-1} r_T} \right)^P + \left(\frac{T^{1-m}}{r_T} \right)^P \right)^{\frac{1}{P}} \quad (2)$$

163
 164 T^* employs the method of modeling tumor growth in [9] (specifically the first term on the right
 165 hand side of equation 1) by having tumor populations transition from exponential to power law growth.
 166 As the authors note, tumors are not able to sustain early exponential growth due to physical and
 167 nutrient limitations. A more appropriate model is where there is exponential growth early which then
 168 transitions to a power law growth at larger tumor sizes. The size at which this transition in growth occurs
 169 is T_{trans} and the smoothness of this transition is governed by the exponent P . The growth term r_T
 170 represents the growth rate and how aggressively the tumor is developing.

171 The second term of Eq. (1) on the right hand side represents the tumor loss due to killing by
 172 CTLs. The parameter k_0 represents the CTL cytotoxic efficacy, with the actual tumor kill rate being
 173 dependent upon the relative numbers of tumor and effector cells $\left(\frac{TE}{T+E}\right)$. However, this rate is mitigated
 174 by the presence of Tregs, with B representing their inhibition efficacy. As Tregs increase in density, the
 175 CTL-mediated tumor death rate decreases.

176
 177 **Effector T cell dynamics**

178

$$\frac{dE}{dt} = \underbrace{H(t_{off} - t)}_1 \underbrace{\left(1 - \frac{M + N}{K_{max}}\right)}_2 \underbrace{\gamma \alpha \frac{TM}{T + M}}_3 - \underbrace{H(t - t_{off})}_{4} \underbrace{\delta_E E \left(1 + c \frac{R}{R + E}\right)}_5 - \underbrace{\rho E}_6 \quad (3)$$

179

180

181

182

183

184

185

186

187

188

189

190

191

192

193

194

195

196

197

198

199

200

201

202

Memory T cell dynamics

$$\frac{dM}{dt} = \underbrace{r_M M \left(1 - \frac{M + N}{K_{max}}\right)}_1 - \underbrace{H(t_{off} - t)}_2 \underbrace{\left(1 - \frac{M + N}{K_{max}}\right)}_3 \underbrace{\alpha \frac{TM}{T + M}}_4 + \underbrace{H(t - t_{off})}_{5} \underbrace{\delta_E \omega E}_{6} \quad (4)$$

203

204

205

206

207

208

209

210

211

212

213

214

215

Memory cells continually replenish themselves through homeostatic growth in term 1. Parameter r_M is the maximum memory T-cell growth rate, which is decreased as the memory and naïve cell numbers reach their carrying capacity, K_{max} . During the immune expansion phase (terms 2-4), there is memory cell loss as they are converted to CTLs. The conversion rate is governed in term 4 by the relative abundances of tumor and memory cells, $\frac{TM}{T+M}$, as well as the antigenicity, α , as mentioned above. As described in Eq. (3), the rate of recruitment is moderated by the relative homeostasis level of the overall immune system. During the contraction phase, memory cells are replenished from the CTL compartment. A fraction (ω) of the CTL are successfully converted back to memory cells [12]. Due to some loss and inefficiency of conversion, the fraction, ω , is less than the loss from the effector cell compartment, $\rho > 0$ [13].

Regulatory T cell and naïve T cell dynamics

$$\frac{dR}{dt} = \sigma T - \delta_R R \quad (5)$$

216

217 Tregs are recruited due to secretion of factors such as TGF-beta from peripheral precursor cells by
 218 tumor cells with recruitment rate σ , and decay with a rate δ_R [14].

219
 220

$$\frac{dN}{dt} = r_N N \left(1 - \frac{M + N}{K_{max}} \right) \quad (6)$$

221 Naive T cell dynamics are largely the result of homeostatic proliferation up to a common carrying
 222 capacity of K_{max} , which is the maximum number of memory and naïve T cells in the immune system [15].
 223 The naive cell replenishment rate is determined by r_N .

224
 225
 226 The model was parameterized based on literature sources when possible, as shown in Table 1. For many
 227 cases there was evidence of variation in parameters, as well as no clear study of each individual
 228 parameter in our model. This is, in part, due to approach to simplify, mathematically, certain processes
 229 in favor of focusing on the tumor-immune dynamics. Where possible, we have tried to make a
 230 biologically reasonable order-of-magnitude approximation. In order to address this parameter
 231 uncertainty we explicitly consider the impact of parameter variation on model results.

Parameter	Symbol	Value	Literature reference
Tumor Growth Coefficient	r_T	1000 cells ⁻¹ day ⁻¹	Robertson-Tessi <i>et al.</i> , 2012
Effector cell kill rate	k_0	1 day ⁻¹	Diefenback <i>et al.</i> , 2001
Regulatory cell suppression efficacy	B	0.75	Robertson-Tessi <i>et al.</i> , 2012
Tumor growth transition size	T_{trans}	10 ⁶ cells	Robertson-Tessi <i>et al.</i> , 2012
Power-Law growth exponent	m	0.5	Robertson-Tessi <i>et al.</i> , 2012
Exponential to power smoothing term	P	3.0	Robertson-Tessi <i>et al.</i> , 2012
Time till immune contraction	t_{off}	5 days	Althaus <i>et al.</i> , 2007
Maximum sustainable number of effector, naïve, and memory cells	E_{max}	10 ¹² cells	Bains <i>et al.</i> , 2009
Tumor antigenicity	α	1*	Robertson-Tessi <i>et al.</i> , 2012
Effector cell death rate (expansion)	ρ	0.0-0.1*	Vignali <i>et al.</i> , 2008
Effector cell death rate (contraction)	δ_E	0.13	Althaus <i>et al.</i> , 2009
Effector cell death rate due to regulatory T cells	c	0.01*	Robertson-Tessi <i>et al.</i> , 2012
Memory cell expansion factor	γ	100*	Althaus <i>et al.</i> , 2007; Arstila <i>et al.</i> , 1999
Tumor-mediated regulatory cell recruitment rate	σ	0.01	Antony <i>et al.</i> , 2005; Robertson-Tessi <i>et al.</i> , 2012
Regulatory cell death rate	δ_R	0.1*	Robertson-Tessi <i>et al.</i> , 2012
Memory cell growth rate	r_M	0.01 day ⁻¹ *	Bains <i>et al.</i> , 2009
Memory cell reconversion rate	ω	0.01*	Bains <i>et al.</i> , 2009

Naïve cell growth rate	r_N	0.1 day^{-1}	Bains <i>et al.</i> , 2009
Maximum number of naïve T cells	K_{\max}	10^{12} cells	Lythe <i>et al.</i> , 2016
Baseline chemotherapy strength	C_0	Varied in simulation	

232 **Table 1:** Model parameters were estimated based upon both pre-existing models, chiefly Althaus *et al.*,
 233 2007 and Robertson-Tessi *et al.*, 2012, as well as experimental studies. For most of the parameters, the
 234 literature often indicated significant variation and so order-of-magnitude approximations were made.
 235 Similarly, certain parameters were not succinctly captured in literature studies and were therefore
 236 estimated (*). We have addressed the impact of potential parameter variation through sensitivity
 237 studies (see Results).

238

239 Simulating chemotherapy and evaluating outcomes

240

241 To establish tolerance in the system and allow transients from initial conditions to dampen before
 242 applying therapy, the simulation was started with a tumor size of 10^7 cells. Chemotherapy was started
 243 when the tumor reached 10^8 cells and was simulated as periodic doses of cytotoxic therapy at 14 day
 244 intervals (a standard cycle length). In total, 10 cycles of chemotherapy were applied. At the time of each
 245 treatment cycle, all cell populations (immune and tumor) were instantaneously reduced by a fraction
 246 representing the cytotoxic effect of chemotherapy. Immune cells were reduced by the same baseline
 247 fraction (C_0) on each cycle. To account for tumor resistance to therapy, the fractional tumor reduction
 248 for cycle i (C_i) was linearly reduced with each cycle, such that the cytotoxic fraction on the last cycle was
 249 75% of C_0 . Approximating the impact of chemoresistance on drug efficacy is challenging since values
 250 vary for different classes of drugs. To further complicate resistance impacts, Hao *et al.* in [16] noted
 251 dose-dependent differences between resistant and resensitized prostate cancer cell populations to
 252 docetaxel (Figure 2, Panel A). The relative advantage of resistant to sensitive cells varied from almost
 253 nothing (at very low doses) to a 400% difference. The value of 75% chemotherapy efficacy at resistance
 254 represents a 33% advantage of survivorship for a resistant population versus a susceptible population. It
 255 is a conservative estimate of the impact of resistance, but we believe it is reasonable given that tumor
 256 populations are unlikely to be entirely homogeneously resistant. Varying this range is a relevant
 257 question for future research. For our purposes, C_i is given by:

258

$$C_i = C_0 \left(1 - 0.25 \frac{i}{10} \right) \quad (7)$$

259

260 The final tumor size after 10 cycles of chemotherapy was compared to the tumor size at the
 261 start of treatment (10^8 cells) and evaluated according to RECIST categories. Specifically, a total loss of
 262 tumor (<-99% change in size) is a complete response (CR). A change between -30% and -99% is
 263 considered a partial response (PR). Tumor changes between -30% and +20% are classified as stable
 264 disease (SD) and changes of greater than +20% are seen as progressive disease (PD) [17]. While there
 265 are many different methods of measuring therapy efficacy impact on disease, RECIST categories were
 266 chosen here since they have correlated well with overall survival in patients across a variety of cancers.

267

268 Simulation environment

269 The model was programmed in the Python language (ver. 2.7.11). The open-source packages Scipy (ver.
 270 0.17.0), Numpy (ver. 1.10.4), and Matplotlib (ver. 1.5.1) were used for simulation of the ODEs as well as
 271 visualization of the results. The platform for the program was both an Intel(R) Core (TM) i7-6820 HQ

272 processor as well as the high performance computing cluster at Moffitt Cancer Center, Tampa, Florida,
273 USA.

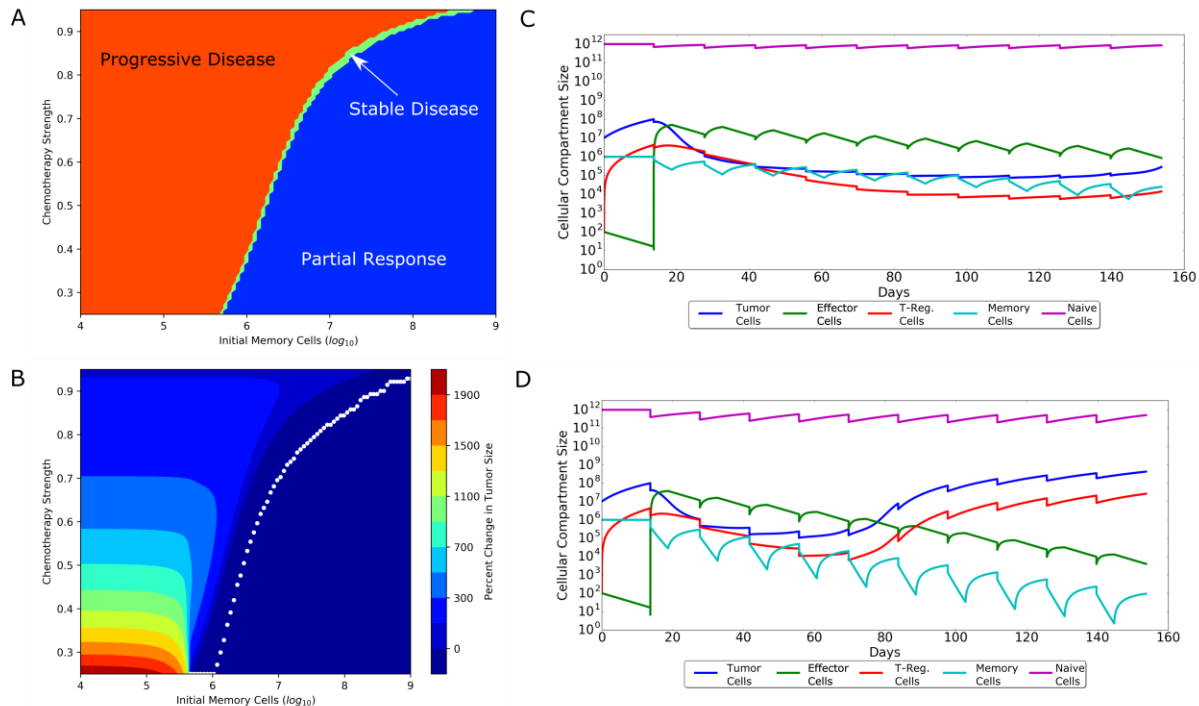
274 Results

275

276 *Influence of patient memory cell populations*

277

278 To analyze the effect of the memory T-cell population on therapy, varying doses of chemotherapy were
279 simulated for a range of memory cell population sizes. The size of the memory T-cell population at the
280 time of therapy was a significant factor affecting the optimal therapeutic response. Memory cell
281 population sizes are variable among patients; Arstila et al. (1999) have estimated there to be $10^6 - 10^7$
282 memory T cell clones in the human body with approximately 10^5 memory T cells per antigen [9, 18].
283 However, due to antigen responses being polyclonal, this suggests multiple orders of magnitude of
284 potential variation in memory T-cell numbers. Patient memory-cell numbers influence the maximum
285 chemotherapy dose strength before treatment failure (Figure 2). Generally, there is a minimum
286 memory-cell population size that is necessary for any given strength of chemotherapy to be successful.
287 Above this threshold, the more memory cells there are, the better the improvement with stronger doses
288 of therapy. Conversely, this means that when memory-cell populations are close to the minimum
289 threshold, chemotherapy should be similarly weak if a more favorable treatment outcome is desired. If
290 memory cells are below the minimum threshold, then the optimal strategy is to use strong
291 chemotherapy (Figure 2, panel A and B). This treatment solely relies on chemotherapeutic cytotoxicity
292 with no immune stimulation.



293
294 **Figure 2:** Interaction of memory-cell populations and chemotherapy strength on treatment outcomes.
295 RECIST outcomes are shown in panel A with progressive disease (red), stable disease (yellow), partial
296 response (light blue) and complete response (dark blue). (B) Finer grade responses are shown as percent
297 changes in tumor size after therapy versus the initial starting size (10^8 cells). The underlying dynamic
298 reasons for these differences can be seen in the memory populations during low (C) and high dose
299 chemotherapy (D). Low dose chemotherapy allows memory populations (light blue) to be sustained for

300 longer and generate larger CTL responses (green). High dose chemotherapy, however, depletes memory
301 cells faster and leads to declining CTL responses and concurrent tumor escape.

302
303 The double-edged nature of chemotherapy on the immune system can be better understood through
304 the transient dynamics during therapy (Figure 2, panel C and D). In cases with stronger chemotherapy
305 dosing, there is an early decrease in tumor population levels as the cytotoxic strength of the therapy
306 comes to bear on cancer populations. However, we observe a trend in that these therapies tend to lead
307 to failure and larger final tumor sizes than if treated with a 'weaker' chemotherapy regimen. Weaker
308 chemotherapy regimens exert lower cytotoxic burdens on the tumor but maintain tumor size reduction
309 for the duration of therapy.

310
311 This counterintuitive result stems from the fact that cytotoxicity alone is insufficient for suppressing
312 tumor growth, especially due to the accumulating chemoresistance. Rather, it is the synergistic effect of
313 cytotoxicity as well as the breaking of immune tolerance and consequent recruitment of CTLs that keeps
314 tumor populations in check. Our *in silico* treatments consistently show that there is an inherent
315 disadvantage to high-dose chemotherapy. There is a gradual decrease in the CTL population over
316 multiple rounds of treatment due to the net loss that stronger dosing causes in memory T-cell
317 populations. It is these memory cells that are affected the most by chemotherapy since they can only
318 recover relatively slowly. If the cytotoxic pressure on memory cells is greater than the recovery rate of
319 that compartment, then even with a resensitized immune system, expansion will lead to fewer CTLs and
320 ultimate treatment failure. In contrast, if the immunodepleting side effects of chemotherapy can be
321 balanced with immune recovery, then more sustainable treatment responses are possible. In short,
322 there is a tradeoff between having chemotherapy strong enough to sufficiently break tolerance, but
323 mild enough to leave sufficient memory T cells for adequate CTL expansion. Akin to the story of
324 Goldilocks and the three bears, the balancing of these two immunological goals leads to an intermediary
325 chemotherapy strength that is 'just right'. *In silico* simulation shows that this "Goldilocks Window" is
326 highly dependent upon patient-specific, pre-existing memory T-cell populations.

327

328

329 **The impact of CTL efficacy**

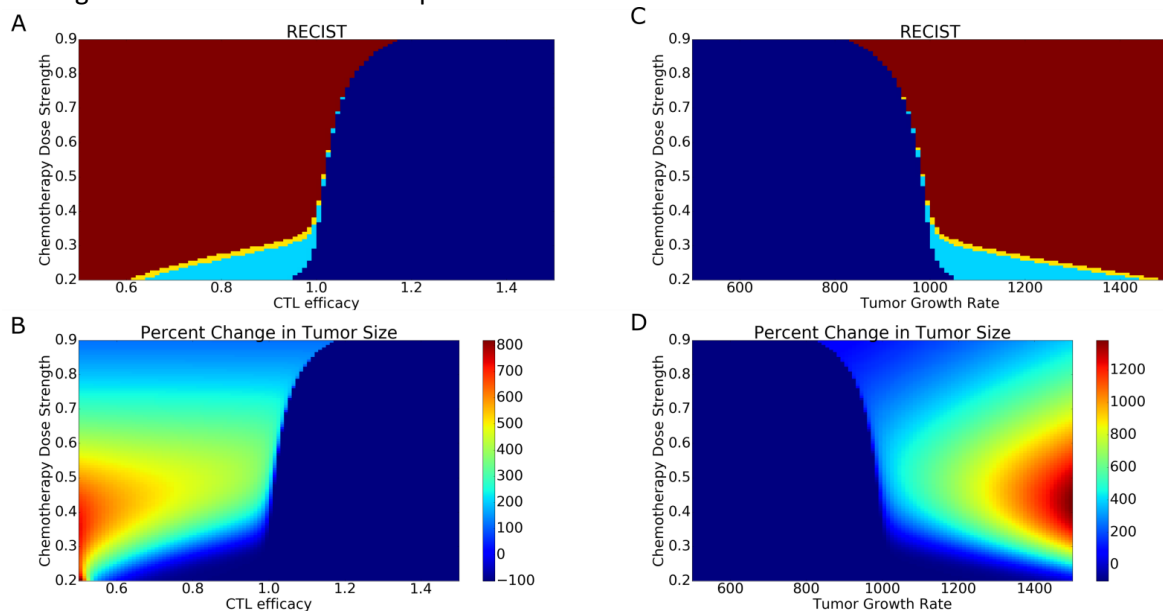
330

331 We sought to identify other relevant patient-specific immune parameters by studying the effect of CTL
332 killing efficacy (k_0). With memory-cell sizes set at 10^6 cells, the cytotoxicity rate was varied around the
333 biologically realistic parameter of 0.9 per day [19]. Unsurprisingly, CTL efficacy is a significant
334 determinant of treatment success (Fig. 1). Furthermore, CTL efficacy dramatically impacts optimal
335 chemotherapy dosing. Lower rates of CTL-mediated tumor cell death require weaker chemotherapy for
336 more favorable treatment outcomes. As before, the underlying dynamics demonstrate the importance
337 of a large enough memory-cell pool over the course of therapy to supply the CTL pool in sufficient
338 numbers. With a lower value of k_0 , more CTLs are necessary to exert the same degree of immune
339 control over the tumor. This in turn, necessitates a larger pool of memory T cells. Strong chemotherapy
340 on a system with lower k_0 values would prevent sufficient CTL expansion by rapidly diminishing the
341 memory-cell populations. This is counterintuitive since an initial motivation may suggest that, in a
342 situation where a patient has a weaker immune system to combat the cancer, the chemotherapy should
343 be increased in order to compensate. However, our model suggests that the lymphodepleting impact of
344 heavy chemotherapy on an already weaker immune system will only worsen outcomes.

345

346 **Impact of tumor growth rates**

347 Tumor growth rates are variable, and in the model we used a value of $r_T = 1000 \text{ cell}^{-1}$ per day, putting
348 growth at a doubling time of 1 day during the fastest exponential growth phase. Experimental and
349 model analyses have shown that selection pressures on growing tumors can lead to significant
350 heterogeneity in metabolism and growth rates [20]. Analysis of the model with different tumor growth
351 rates revealed that optimal dosing was dependent on this variation (Fig. 3). For slower growing tumors,
352 greater doses can be used because chemotherapeutic cytotoxicity is sufficient for controlling tumor
353 growth. For faster growing tumors (larger r_T) it becomes necessary to decrease chemotherapeutic
354 strength in order to achieve optimal outcomes; chemotherapeutic cytotoxicity is insufficient alone and
355 so CTL-mediated tumor death is necessary. Greater CTL involvement, though, imposes the same trade-
356 off as above, in that dosing must be weakened in order to sustain memory cell populations. Importantly,
357 for the most aggressively growing tumors, there is actually a 'worst-case scenario' of intermediary
358 chemotherapy strength. Here, the worst chemotherapy is not, in fact, the strongest possible dose and is
359 instead a 'mid-range' strength in treatment. At this chemotherapeutic strength, the drug alone is
360 insufficient to cause a reduction in tumor size. However, the dose is still strong enough to lead to severe
361 memory cell population depletion and undermines any immune efforts at constraining tumor growth.
362 These considerations demonstrate how the tumor growth rate is a primary determinant of tumor
363 control and, depending on the individual patient's tumor, determines which dynamics are capable of
364 leading to successful treatment responses.



365 **Figure 3:** Treatment outcomes for variation in CTL efficacy (A and B) and tumor growth rate (C and D).
366 Panels A and C represent RECIST outcomes. Red is progressive disease (PD), dark blue is complete
367 response (CR), light blue is partial response (PR) and yellow is stable disease (SD). As CTLs become more
368 efficient at killing tumor cells, there is a dramatic reduction in final tumor size and a significant
369 improvement in outcome. However, below a threshold efficacy, chemotherapy has a much more
370 important role in impacting the role of therapy. Weaker chemotherapy leads to better outcomes. A
371 similar pattern is shown in response to variation in tumor growth rates. Faster growing tumors lead to
372 significantly poorer treatment outcomes. This trend is most observable when, for chemotherapy values
373 below 0.4, the range of tumor growth rates and CTL efficacies where tumor reduction is possible
374 significantly increases. Chemotherapy plays an important modulating role in these faster growing
375 tumors, however, with optimal treatment coming from weaker chemotherapy.
376
377

378 In short, patient immune biology determines optimal chemotherapy strength by determining which
379 immune dynamics can be taken advantage of to control tumor growth. Low dose therapy is optimal in
380 situations where the patient immune response is robust enough to control tumor growth. This requires
381 both a sufficient memory-cell population as well as sufficiently high efficacy in CTL cytotoxicity. In
382 contrast, high-dose chemotherapy is optimal to control tumor growth when either the immune system
383 is unable to generate a sufficient CTL response, or when the tumor is slow-growing. However, in many
384 situations where the immune system is able to enhance the effect of chemotherapy, dosing must be
385 moderated so that it does not impose an overly large recovery burden and impede immune effects.
386

387 Improvements to therapy outcomes from immunostimulatory vaccines: The Goldilocks Window

388
389 Patient-specific vaccines have become a recent hallmark in personalized cancer therapy. One of the first
390 to acquire FDA approval was Sipuleucel-T, for treating metastatic castrate resistant prostate cancer [21].
391 Each vaccine is tailored to a specific patient by culturing dendritic cells from patient serum samples
392 (taken roughly 72 hours before vaccine administration). The goal is to activate dendritic cells *in vitro*
393 with a specific tumor protein target. These cultured antigen-presenting cells are then injected into the
394 patient in order to stimulate an antitumor immune response. Three doses were administered in 2 week
395 intervals with significant clinical responses being observed. Vaccination led to a 22% reduction in the
396 relative risk of death, although there was no noticeable decrease in the rate of progression of disease
397 [21]. The specific effect on T cells has been quantified by looking at T-cell receptor changes in response
398 to vaccination. Subjects that received the vaccine saw a change in abundance and diversity of T-cell
399 receptors in tumor-infiltrating lymphocytes. Certain receptor sequences were enriched, while others
400 were significantly decreased [22], suggesting that the vaccine promoted an antigen-specific immune
401 response against the tumor.

402 To study the effects and potential synergy of chemotherapy with this method of T-cell stimulation, we
403 simulated a vaccine regime similar to that used for Sipuleucel-T (3 doses, spaced 14 days apart), with
404 different vaccine strengths. Mathematically, this was modeled by modifying the ODEs that govern CTL
405 expansion. The antigenicity parameter of the tumor, α , was changed from a constant coefficient to a
406 variable, time-dependent function, $\alpha_v(t)$:

$$\alpha_v(t) = \alpha + v \left(\frac{1}{2} \right)^{\frac{t}{t_{half}}} \quad (9)$$

407
408 Total antigenicity is modeled as the result of both the constant, baseline antigenicity of the tumor, α ,
409 and the exponentially decaying vaccine-augmented component, v . Vaccine-augmented antigenicity
410 decays with a half-life, t_{half} , of 3 days, a biologically realistic timespan in line with the short half-lives of
411 dendritic cells [23]. This model of dynamic antigenicity can be expanded for multiple vaccinations, as
412 used in the clinical protocol (eq. 10).

$$\alpha_v(t) = \alpha + \sum_{n=1}^{n_{vac}} H(t - t_n) v \left(\frac{1}{2} \right)^{\frac{t-t_n}{t_{half}}} \quad (10)$$

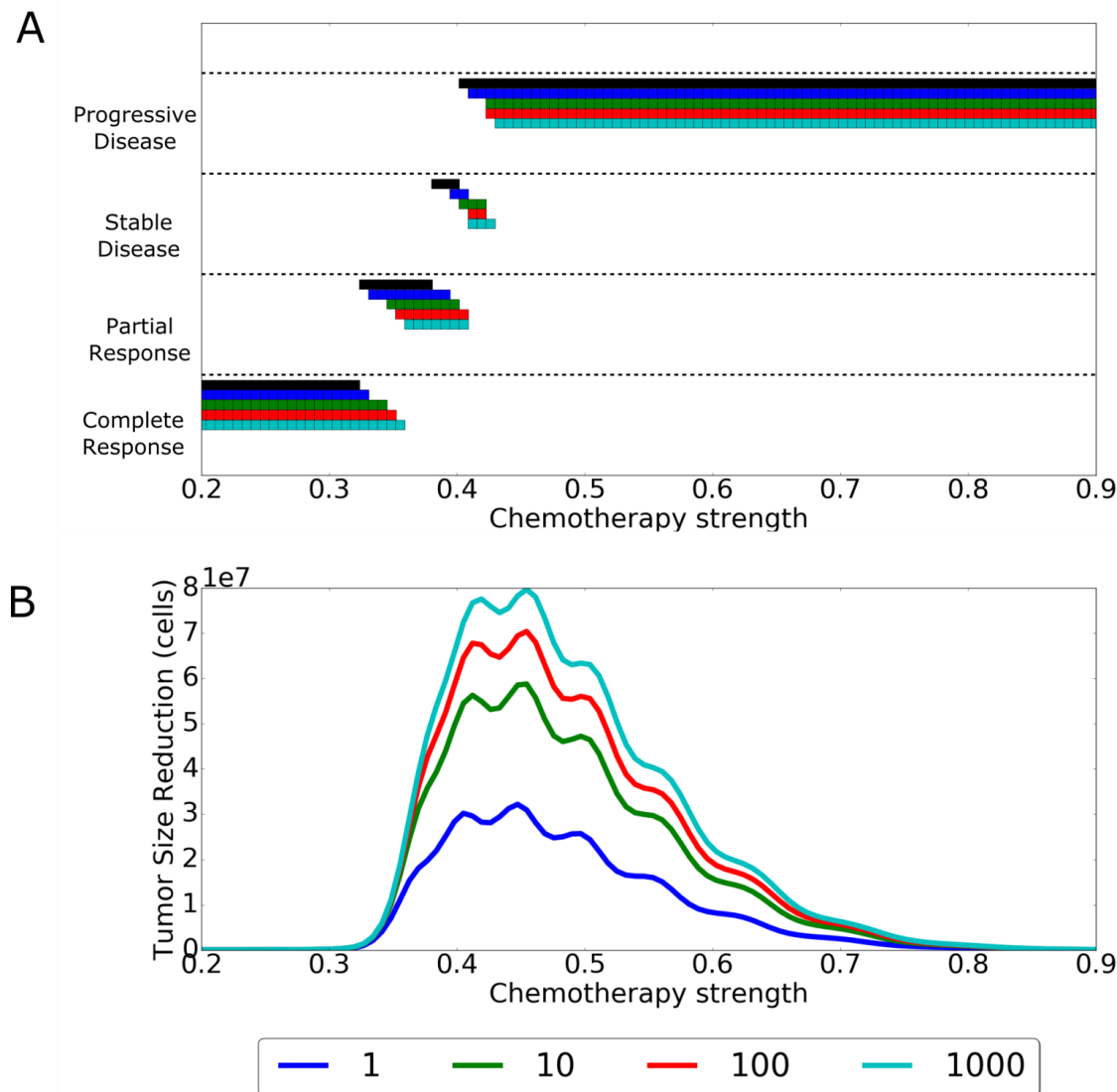
413
414 Here, $H(t)$ is again the Heavyside function. n_{vac} represents the total number of vaccine injections and t_n
415 represents the time of the n^{th} vaccination.

416 The ODEs used for the simulation of immune and tumor cell populations are then dependent on the
417 instantaneous current value of $\alpha_v(t)$ throughout the course of simulated therapy.

418 Under this scheme, results show that vaccine therapy can improve outcomes, but only within a specific
419 range of chemotherapy strengths (Fig. 4). For very high chemotherapy doses, the beneficial effects of a

15

420 vaccine are diminished. As before, the underlying cause for decreasing efficacy is the persistent
421 lymphodepletion of memory cells due to the chemotherapy. Antigenicity augmentation due to vaccine
422 stimulation is offset by reduced CTL expansion. However, very low-dose chemotherapy poses its own
423 challenges, because with insufficient lymphodepletion, tolerogenic mechanisms and greater Treg
424 recruitment inhibit any CTL response augmented by the vaccine. The immune system remains closer to
425 tumor-tolerized homeostasis, and as a result vaccine stimulation is mitigated because the immune
426 system is already suppressed.
427



428
429 **Figure 4:** Improvements in tumor reduction due to vaccine application. Panel A shows the RECIST
430 responses achieved for different vaccine strengths and chemotherapy strengths with black being the
431 non-vaccine baseline. Vaccine strengths (v) are 1 (blue), 10 (green), 100 (red), 1000 (light blue). Larger
432 vaccine strengths lead to more successful RECIST responses for stronger chemotherapy doses. When
433 looking at the absolute number of improvement in cellular reduction (B), a window of optimal
434 chemotherapy ranges appears. Only when chemotherapy is in this range can vaccines provide a
435 significant additional benefit.
436

437
438 Therefore, there exists an optimal dosing window for chemotherapy, a “Goldilocks” window.
439 Quantitatively, we define this window to be the region in which a therapy dose can offer at least a 20%
440 reduction in tumor size since this is the necessary amount for disease to become classified as a partial
441 response. In order for there to be this maximized benefit from vaccine application, the chemotherapy
442 regimen must be ‘just right’. Chemotherapy must have sufficient lymphodepletion to resensitize the
443 immune system, but must leave enough immune cells such that vaccine stimulation leads to a large CTL
444 response. Similar to the results of chemotherapy without the vaccine, the specific range of this
445 Goldilocks window depends upon the initial patient memory cell (M_0) numbers (not shown). More
446 memory cells mean a system able to tolerate a larger dose of chemotherapy and still lead to a large
447 vaccine-triggered CTL response. In contrast, fewer memory cells requires weaker chemotherapy doses
448 to derive a maximum benefit from vaccine administration.

449
450 **Impact of variation in immune support**

451
452 Chemotherapeutic lymphodepletion in the clinical setting can pose a serious threat to the safety of the
453 patient through neutropenia [24], which commonly leads to dose reductions and disruptions to the
454 standard schedule of therapy for patients. Consequently, multiple tools have been developed to help
455 mitigate the effects of chemotherapy on the immune system. For example, it was recognized that
456 dexamethasone treatment before carboplatin and gemcitabine could not only increase chemotherapy
457 efficacy but also reduce the lymphodepleting effects by preventing uptake in the spleen and bone
458 marrow [25]. In contrast, other aspects of cancer therapy can potentially hamper CTL responses to
459 tumor insults. For example, G-CSF application has been shown to reduce $CD8^+$ T cell activation and could
460 conceivably impede the impact of lymphodepletion as a break from immune tolerance [26]. More
461 generally, however, the broader impact of immune system augmentation or suppression during therapy
462 remains unexamined.

463 In order to examine the effect of attenuated or augmented lymphodepletion on therapy outcome, we
464 allowed for variable chemotherapeutic toxicity to immune populations, as compared to the tumor
465 population. Mathematically, this simply means modifying the chemotherapy dose by a scaling factor h .
466 The effect of chemotherapy on immune cell populations at a given treatment time is:

$$I_1 = I_0(1 - hC) \quad (8)$$

467
468 where I_1 is the immunological population size after application of chemotherapy, I_0 is the population size
469 before therapy, and $0 < C < 1$ is the dose strength. The specific numerical range in which h falls
470 represents either attenuated or augmented chemotherapeutic toxicity. For values of $0 < h < 1$, this
471 represents an attenuated toxicity relative to the toxicity on the tumor. In contrast, values of $h > 1$
472 represent higher toxicity on patient immune populations than on the tumor. This could be due to
473 patient-dependent increased sensitivity to chemotherapy. However, this is really beyond the scope of
474 our model, especially since mathematically I_1 could become negative. This is clearly an area where our
475 model may not accurately capture the dynamics. Therefore, we have restricted hC such that $hC < 1$. For
476 our *in silico* therapies, h was varied across these ranges where $I_1 > 0$ for three different strengths of
477 treatment. Values of C were chosen to represent lower ($C= 0.25$), middle ($C= 0.6$), and higher ($C= 0.9$)
478 dose chemotherapy.

479 Outcomes of therapy due to variation in h depended upon the strength of chemotherapy.
480 Interestingly, the results suggest that immune-supporting combination therapy has essentially no
481 benefit when given with low dose chemotherapy. As shown in Figure 5, similar tumor reduction
482 occurred for a wide range of values of h around $h=1$ (which represents no immune support).

483 Furthermore, outcomes were worse when h was very low or very high. In situations where it was very
484 low, final tumor sizes were large because a lack of lymphodepletion did not sufficiently break immune
485 tolerance. In contrast, for larger h values, there was over-depletion which prevented an effective T-cell
486 response despite significant tolerance breaking.

487 In contrast, high dose chemotherapy saw treatment failure or success highly dependent upon
488 the amount of immune support. Similar to low dose therapy, a small value of h that mitigated the
489 depleting effects of chemotherapy led to the best possible outcomes in terms of tumor shrinkage. Final
490 tumor sizes were, in fact, multiple orders of magnitude lower than was possible with low-dose
491 chemotherapy. As h increased (representing less toxicity mitigation) treatment outcomes rapidly
492 worsened. The transition value h^* , where the clinical outcome rapidly shifts, indicates a threshold effect
493 with regard to immune support. For high chemotherapy doses, immune support treatments must have a
494 significantly large mitigation ($h < h^*$) of immunodepletion in order for successful treatment responses to
495 occur.

496 Interestingly, the moderate strength chemotherapy regimen yielded only partial benefits of
497 either extreme. The greatest tumor reduction possible, with immune support, yielded tumors that were
498 smaller than those achievable with low dose chemotherapy. However, these tumors were still multiple
499 orders of magnitude larger than those achievable with high dose chemotherapy. For treatment failure at
500 lower immune support ($h > h^*$) tumor sizes were actually larger than when high dose chemotherapy
501 failed.

502 Clinically, the results suggest that chemotherapy dose strength can be used to mitigate
503 uncertainty regarding the amount of immune support a certain treatment will give to a specific patient.
504 Low dose therapy offers a wide range of potential immune support in which treatment can successfully
505 reduce tumor sizes. The disadvantage is that the maximum tumor size reduction still leaves larger
506 tumors than are possible using higher doses of chemotherapy. While our model has not analyzed this, a
507 potential impact is that larger tumor sizes could lead to more heterogeneous populations and thus lead
508 to a higher likelihood of resistant or metastatic populations. However, higher doses have a narrower
509 range of immune support in which they are successful. Chemotherapy can be balanced, then, against
510 how certain the clinician is of the benefit that G-CSF (or other immune supporting drug) will give. For
511 patients where there is high certainty of a significant benefit due to the drug, high dose therapy is
512 optimal. In contrast, lower dosing should be used when the drug may have lower or variable efficacy.
513

514 **Variable Immune Support and Impacts on Observed Cohort Responses**

515
516 Finally, we sought to investigate how variation in the effectiveness of these immune adjuvants
517 might impact treatment outcomes in a group of patients. Chemotherapy treatment leads to a wide
518 range of responses, both successful and unsuccessful, across multiple types of cancer [17]. This variation
519 has been attributed to both disease variation, patient variation, and interactions between the two.
520 However, less attention has been given to variable patient responses to secondary drugs – such as G-CSF
521 – and how they impact therapy. Patient responses to these secondary drugs are currently poorly
522 measured and could have significant implications for therapy outcomes.

523 To better explore the effect of variable patient responses to immune support drugs, cohorts of
524 500 patients were randomly generated from a normal distribution with a mean immune support
525 response value of $h = 0.8$ and variance of 0.2. These values were chosen to center the distribution
526 around the model-derived threshold value $h^* = 0.8$. Similar to our previous investigations, cohorts were
527 then subjected to regimens of low ($C = 0.4$) and high ($C = 0.8$) chemotherapy strengths. Percent changes
528 in tumor size after therapy were displayed for each individual patient in the cohort to generate a
529 waterfall plot. In doing so, we used our model to simulate cohort responses as is commonly measured in
530 aggregated studies of patient data [17]. The waterfall plots (Fig. 5) illustrate that chemotherapy strength

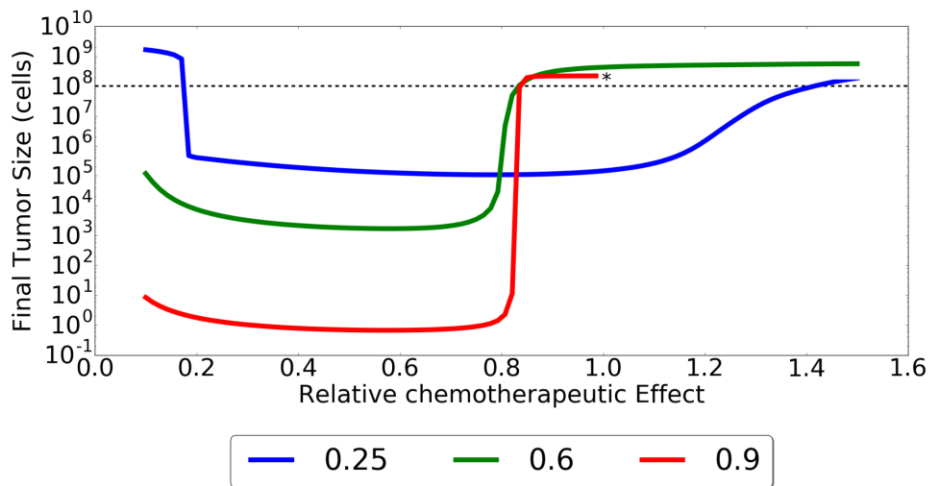
531 can significantly change the proportion of successfully responding patients in a population with variable
532 responses to immune prophylactics. This is significant since the proportion of successful responses is
533 often an important criterion for judging therapeutic efficacy. The simulated waterfall plots show how
534 clinical outcomes could not only be the result of therapy, but also due to inherent immune variation
535 within the cohort.

536

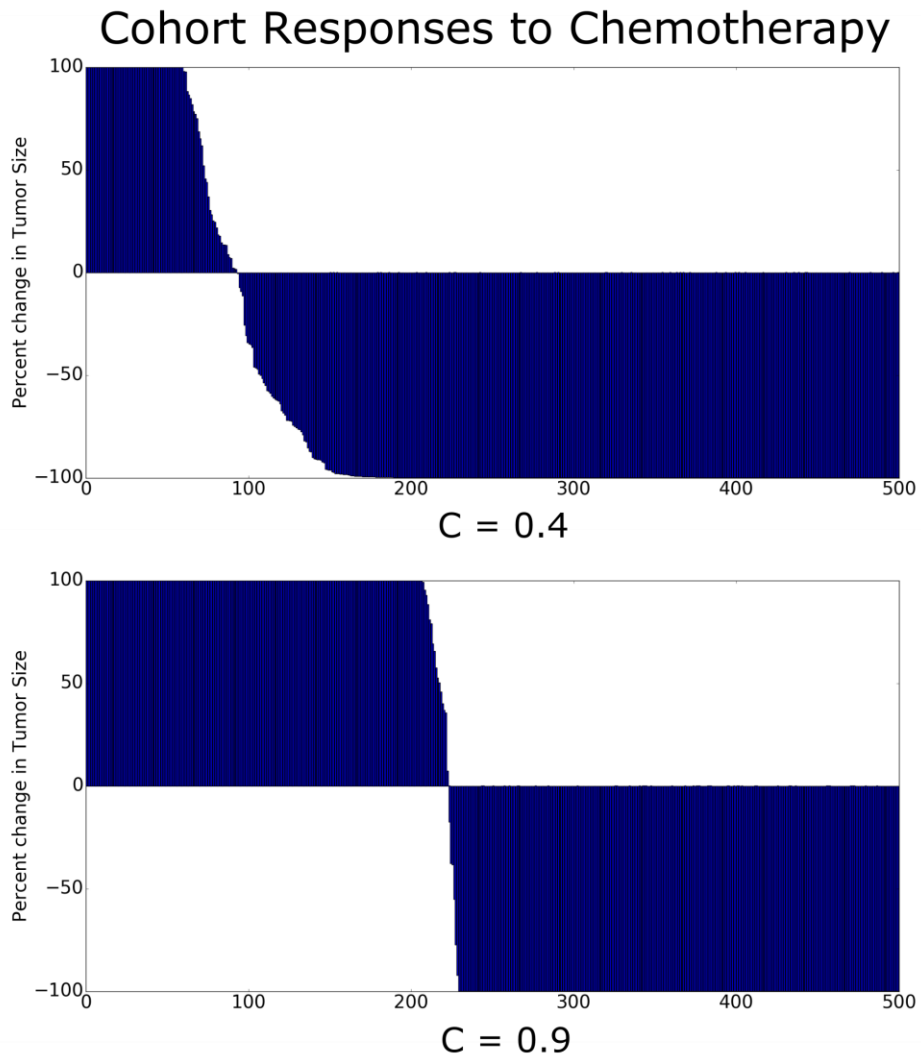
537

19

A



B



539 **Figure 5:** Therapeutic effects of differential response to immune prophylactics. (A) Final tumor
540 sizes are shown for three different chemotherapy regimes for a range of immune modifier efficacies (h).
541 The asterisk denotes that simulations were only run up to this h value for the highest dose
542 chemotherapy. (B) Cohorts are treated with these differing regimes of high and low chemotherapy,
543 showing significant differences in the proportion of successful versus unsuccessful responders.

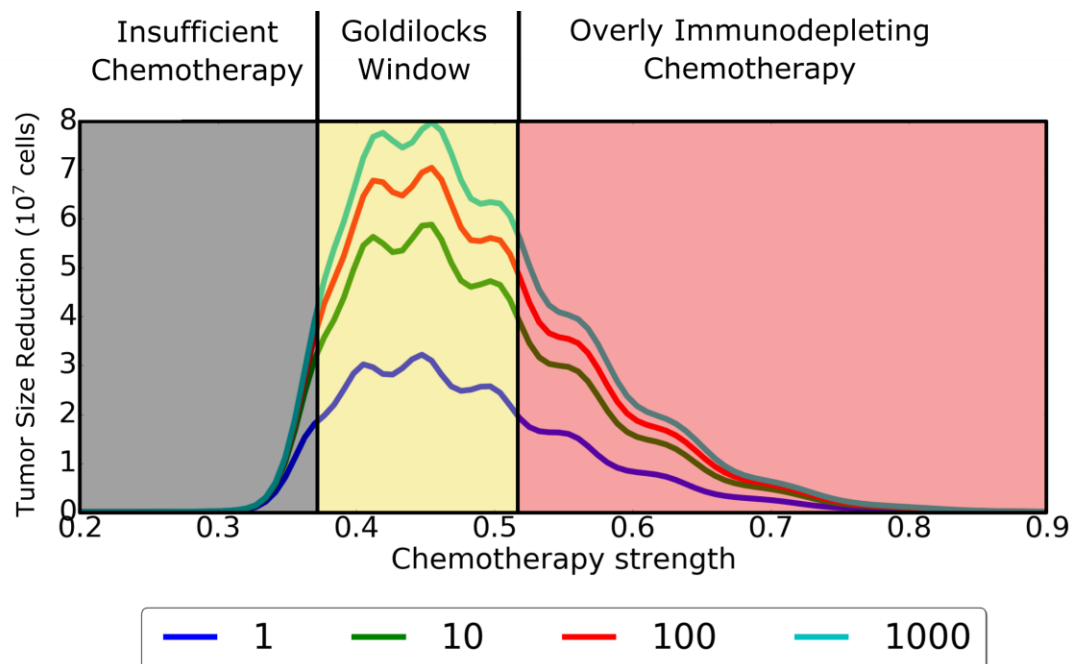
544

545 Discussion

546 A major barrier to success for immunotherapy in cancer is tolerogenic mechanisms that reduce the
547 immune response to tumor antigens ([27], [3], [6]) . A potential solution has come from observations
548 that lymphodepletion stimulates homeostatic proliferation in the immune system which can transiently
549 restore immune response. This has led to increasing efforts to selectively apply chemotherapy to
550 improve outcomes from immunotherapy [28].

551

552 To better understand this potential synergy, we constructed a mathematical model to frame these
553 complex dynamics and identify critical parameters that govern the clinical outcomes. Our studies
554 focused on three clinically-observed dynamics of immunodepletion, immunostimulatory vaccination,
555 and immunosupportive prophylactics. With regard to immunodepletion, we demonstrated that
556 chemotherapy results in a trade-off. At very high doses, chemotherapy has a maximal cytotoxic effect on
557 the tumor but also maximally depletes memory T cells such that no effective CTL response can be
558 mounted despite the transient loss of tolerance during re-expansion of the immune cells after
559 completion of chemotherapy. Similarly, low doses of chemotherapy are insufficient to produce the post-
560 treatment immune cell expansion that is necessary for reversal of immune tolerance.
561 Importantly, however, we find there is a “Goldilocks” range of chemotherapy doses in which
562 lymphodepletion causes adequate immune re-sensitization, but does not impose an overly large
563 recovery burden. This window is governed by the patient-specific quantity of memory T cells so that
564 larger pre-treatment T-cell populations allow more favorable outcomes with higher doses of
565 chemotherapy. In contrast, fewer pretreatment CTLs can limit the immune response even in the
566 “Goldilocks” range of chemotherapy. Thus, there is a necessary 'minimum efficacy' of effector cells for
567 successful stimulation of immune response by chemotherapy. Below this threshold of immune activity,
568 the benefit of chemotherapy is almost solely dependent on its inherent cytotoxicity (Fig. 6)



569
570 **Figure 6:** A diagram explaining tumor outcomes at varying chemotherapy strengths and immune support
571 doses. If therapy is too weak, then immune stimulation cannot be maximally effective and direct
572 chemotherapy-mediated tumor cell death is also low. This yields a suboptimal tumor reduction. When
573 chemotherapy is too strong, there may be more tumor cell death due to the drug, but insufficient
574 immune activation due to over depletion of T cells. There is a moderate dose, however, that represents
575 a Goldilocks window of maximizing both T-cell activation as well as drug-induced tumor cell death. This
576 range of dosing provides at least a 20% reduction in tumor size (relative to the initial tumor size of 10⁸
577 cells).

578
579 Our model also provides insight into the potential effects of variation in the tumor growth rate. In
580 slower growing tumors, chemotherapy alone can be sufficient to achieve optimal treatment response.
581 Treatment of faster growing tumors, however, is best when the chemotherapy is administered to
582 enhance the immune response. Unfortunately, if the pre-treatment population of CTLs is small, we find
583 chemotherapy for rapidly growing tumors will be ineffective if it is both highly lymphodepleting and
584 insufficiently cytotoxic to significantly reduce tumor growth. Assessing the clinical importance of this
585 question is challenging because it remains unclear from the literature as to the actual size of the
586 population of tumor-specific T cells that are present during treatment. In spite of these difficulties, the
587 impact and existence of anti-tumor immunity has been bolstered by recent immunotherapies which act
588 to remove inhibitions to T-cell action [29].

589
590 Chemotherapy is increasingly being used in concert with vaccines to help stimulate the patient immune
591 system. We investigated the interactions between vaccines and lymphodepletion and found that, as
592 before, there is a window of chemotherapy ranges in which vaccines can improve outcomes versus
593 chemotherapy alone. At very high doses, however, the resulting lymphodepletion substantially reduces
594 benefits of immune stimulation by vaccination. More broadly, other novel immunotherapies could also
595 potentially be hampered by over-depletion of the immune system.

596
597 To further investigate the potential impact of this interaction, we modeled the effect of differential
598 responses to immune prophylactics. G-CSF and other drugs have become common recourses in

599 chemotherapy for mitigating the immunodepletion effects on patients [30]. However, recent studies
600 have suggested that T cell response is hampered by G-CSF administration [26]. While G-CSF may help
601 prevent neutropenia and cytopenia for patients, it may impede the ability of retolerized T cells to mount
602 an anti-tumor response. In addition, responses to prophylactics are not constant but the significance of
603 this variation remains relatively uninvestigated. Our model suggests that inter-patient variation in
604 prophylactic response can lead to drastically different outcomes for the same dosing of chemotherapy.
605 Across larger samples, this variation can further interact with chemotherapy to be a significant
606 determinant of whether the chemotherapy dose leads to more success or failure across a range of
607 patients.

608
609 In conclusion, our results suggest opportunities to increase the efficacy of immunotherapy with precise
610 application of chemotherapy. Our model affirms the importance of effector and memory T-cell
611 expansion following chemotherapy to reduce immune tolerance to tumor antigens. However, we
612 demonstrate that optimal chemotherapy requires identification of a Goldilocks Window in which
613 treatment can both induce cytotoxic effects in the tumor and enhance the immune response to tumor
614 antigens. Identifying optimal strategies for chemotherapy in each patient will likely benefit from the
615 application of mathematical models which are parameterized by patient data pre-treatment to generate
616 an optimal treatment strategy for that patient. Importantly, these predicted strategies would most likely
617 need to change as patient responses diverge from those predicted, leading to an iterative loop of
618 'predict-apply-refine'. With the growing drive towards precision medicine, we believe that mathematical
619 models are critical for the future of truly personalized therapy, where no two patients will receive the
620 same therapeutic regimen, and where treatments adapt a change based on patient responses. The
621 model presented here is a step towards describing the complex landscape of treatment decisions
622 regarding dosing and combination of different therapies, and we have shown how these decisions can
623 be sensitive to patient-specific parameters and guide clinical intuition.

624

625

626 Works Cited

627

- [1] P. Antony, C. Piccirillo, A. Akpınarlı, S. Finkelstein, P. Speiss, D. Surman, D. Palmer, C. Chan, C. Klebanoff, W. Overwijk, S. Rosenberg and N. Restifo, "CD8+ T cell immunity against a tumor/self-antigen is augmented by CD4+ T helper cells and hindered by naturally occurring T regulatory cells," *J Immunol*, vol. 5, no. 174, pp. 2591-601, 2005.
- [2] A. Corthay, "How do Regulatory T Cells Work?," *Scand J Immunol*, vol. 70, no. 4, pp. 326-336, 2009.
- [3] A. Tanaka and S. Sakaguchi, "Regulatory T cells in cancer immunotherapy," *Cell Research*, vol. 27, pp. 109-118, 2017.
- [4] D. Thomas and J. Massgue, "TGF-beta directly targets cytotoxic T cell functions during tumor evasion of immune surveillance," *Cancer Cell*, vol. 8, no. 5, pp. 369-80, 2005.
- [5] S. McKarns and R. Schwarz, "Distinct effects of TGF-beta 1 on CD4(+) and CD8(+) T cell survival, division, and IL-2 production: A role for T cell intrinsic Smad3," *J Immunol*, vol. 174, no. 4, pp. 2071-83, 2005.
- [6] Y. Takeuchi and H. Nishikawa, "Roles of regulatory T cells in cancer immunity," *Int Immunol*, vol. 28, no. 8, pp. 401-9, 2016.
- [7] C. Wrzensinski, C. Paulos, A. Kaiser, P. Muranski, D. Palmer, L. Gattinoni, Z. Yu, S. Rosenberg and N. Restifo, "Increased intensity lymphodepletion enhances tumor treatment efficacy of adoptively transferred tumor-specific T cells," *J Immunother*, vol. 33, no. 1, pp. 1-7, 2010.
- [8] C. Althaus, V. Ganusov and R. De Boer, "Dynamics of CD8(+) T cell responses during acute and chronic lymphocytic choriomeningitis," *J Immunol*, vol. 17, no. 9, pp. 2944-51, 2007.
- [9] M. Robertson-Tessi, A. El-Kareh and A. Goriely, "A mathematical model of tumor-immune interactions," *Journal of Theoretical Biology*, vol. 294, pp. 56-73, 2012.
- [10] L. Gattinoni, S. Finkelstein, C. Klebanoff, P. Antony, D. Palmer and P. Spess, "Removal of homeostatic cytokine sinks by lymphodepletion enhances the efficacy of adoptively transferred tumor-specific CD8(+) T cells," *Journal of Experimental Medicine*, vol. 202, 2005.
- [11] D. A. A. Vignali and L. W. W. C. J. Collison, "How regulatory T cells work," *Nat Rev Immunol*, vol. 8, no. 7, pp. 523-532, 2008.
- [12] W. Cui and S. Kaech, "Generation of effector CD8+ T cells and their conversion to memory T cells," *Immunological Reviews*, vol. 236, pp. 151-66, 2010.
- [13] I. Bains, R. Antia, R. Callard and A. Yates, "Quantifying the development of the peripheral naive CD4(+) T-cell pool in humans," *Blood*, vol. 113, pp. 5480-7, 2009.
- [14] L. E. Richert-Spuhler and J. M. Lund, "The Immune Fulcrum: Regulatory T Cells Tip the Balance Between Pro- and Anti-inflammatory Outcomes upon Infection," *Prog Mol Biol Transl Sci*, vol. 136, pp. 217-243, 2015.
- [15] G. Lythe, R. E. Callard, R. L. Hoare and C. Molina-Paris, "How many TCR clonotypes does a body maintain?," *J Theor Biol*, no. 389, pp. 214-224, 2016.
- [16] J. Hao, M. Madigan, A. Khatri, C. Power, T. Hung, J. Beretov, L. Chang, W. Xiao, P. Cozzi, P. Graham, J. Kearsley and Y. Li, "In Vitro and In Vivo Prostate Cancer Metastasis and Chemoresistance Can Be Modulated by Expression of either CD44 or CD147," *PLoS One*, vol. 7, no. 8, p. e40716, 2012.
- [17] R. Jain, J. Lee, C. Ng, D. Hong, J. Gong, A. Naing and e. al., "Change in Tumor Size by RECIST

- Correlates Linearly With Overall Survival in Phase I Oncology Studies.," *Journal of Clinical Oncology* , vol. 30, pp. 2684-90, 2012.
- [18] T. Arstila, A. Casrouge, V. Baron, J. Even, J. Kanellopoulos and P. Kourilsky, "A direct estimate of the human alpha T cell receptor diversity," *Science*, vol. 286, no. 5441, pp. 958-61, 1999.
- [19] A. Diefenbach, E. Jensen, A. Jamieson and D. Raulet, "Rae1 and H60 ligands of the NKG2D receptor stimulate tumour immunity.," *Nature* , vol. 413, pp. 165-71, 2001.
- [20] M. Robertson-Tessi, R. Gillies, R. Gatenby and A. Anderson, "Impact of Metabolic Heterogeneity on Tumor Growth, Invasion, and Treatment Outcomes.," *Cancer Research* , vol. 75, pp. 1567-79, 2015.
- [21] G. Plosker, "Sipuleucel-T In Metastatic Castration-Resistant Prostate Cancer," *Drugs*, vol. 71, no. 1, pp. 101-8, 2011.
- [22] N. Sheikh, J. Cham, L. Zhang, T. DeVries, S. Letarte, J. Pufnock and e. al., " Clonotypic Diversification of Intratumoral T Cells Following Sipuleucel-T Treatment in Prostate Cancer Subjects," *Cancer Research*, vol. 76, pp. 3711-8, 2016.
- [23] M. Merad and M. Manz, " Dendritic cell homeostasis.," *Blood* , vol. 113, pp. 3418-27, 2009.
- [24] J. Crawford, D. Dale and G. Lyman, " Chemotherapy-induced neutropenia - Risks, consequences, and new directions for its management.," *Cancer*, vol. 100, pp. 228-37, 2004.
- [25] H. Wang, M. Li, J. Rinehart and R. Zhang, "Dexamethasone as a chemoprotectant in cancer chemotherapy: hematoprotective effects and altered pharmacokinetics and tissue distribution of carboplatin and gemcitabine.," *Cancer Chemotherapy and Pharmacology*, vol. 53, no. 6, pp. 459-67, 2004.
- [26] 2. T. S. Bunse CE1, J. Lahrberg, M. Oelke, C. Figueiredo, R. Blasczyk and B. Eiz-Vesper, "Granulocyte colony-stimulating factor impairs CD8+ T cell functionality by interfering with central activation elements," *Clin. Exp Immunol*, vol. 185, no. 1, pp. 107-118, 2016.
- [27] R. Kim, M. Emi and K. Tanabe, "Cancer immunoeediting from immune surveillance to immune escape," *Immunology* , vol. 121, pp. 1-14, 2007.
- [28] A. Makkouk and G. Weiner, " Cancer Immunotherapy and Breaking Immune Tolerance: New Approaches to an Old Challenge.," *Cancer Research* , vol. 75, pp. 5-10, 2015.
- [29] H. Guo and K. Tsung, "Tumor reductive therapies and antitumor immunity," *Oncotarget*, vol. 8, no. 33, p. 55736–55749, 2017.
- [30] H. M. Mehta, M. Malandra and C. S. J, "G-CSF and GM-CSF in Neutropenia," *J Immunol*, vol. 195, no. 4, pp. 1341 - 1349, 2015.
- [31] G. Freyer, N. Jovenin, G. Yazbek, C. Villanueva, A. Hussain, A. Berthune and e. al., "Granocyte-colony Stimulating Factor (G-CSF) Has Significant Efficacy as Secondary Prophylaxis of Chemotherapy-induced Neutropenia in Patients with Solid Tumors," *Anticancer Res*, vol. 33, no. 1, pp. 301-7, 2013.
- [32] L. Bracci, G. Schiavoni, A. Sistigu and F. Belardelli, " Immune-based mechanisms of cytotoxic chemotherapy: implications for the design of novel and rationale-based combined treatments against cancer," *Cell Death and Differentiation* , vol. 21, pp. 15-25, 2014.